Swarm-Cut: A PSO-Based Meta-Heuristic Method for Hotwire Trajectory Planning.

Rollo D. L. Tully, University of Manchester, MAE

Abstract – **The performance of Hotwire tool paths is difficult to calculate due to the nonlinear and multivariable interactions with the kerf width. Accurate cutting requires a balance of trajectory, velocity, and heating to achieve high geometric fidelity. To reduce the complexity we recontextualise the problem. Instead of attempting to predict wire kerf, a problem which has been explored thoroughly but has failed to see real world use, we instead consider it as an energy distribution problem. We introduce a new parameter, Critical Specific Energy (CSE), that quantifies the minimum thermal energy that must be delivered to the surface of a material to achieve ablation. Use of CSE simplifies the thermal-mechanical interaction, and allows for the construction of an indirect optimisation problem. We formulate a bespoke Particle Swarm Optimisation (PSO) meta-heuristic using CSE to minimise surface deviation while considering real world manufacturing constraints. This method termed Swarm-Cut, is applied to a composite sandwich panel wing core, using Swarm-Cut reduced the mean surface deviation from 1.67 mm to 0.53 mm (68.3% reduction) and reduced the standard deviation of surface deviation($\sigma\Delta$) from 1.59 mm to 0.352 mm (77.9% reduction) when compared to baseline trajectories demonstrating gains in both manufacturing consistency, accuracy and simplifying process tuning.**

I. INTRODUCTION

Hot-wire cutting (HWC) is a subtractive manufacturing method that produces components that can be described by ruled surface. Hot-wires remove material by ablation or melting in a region close to the wire. The size of the ablated region is dependent of a large number of independent parameters, including, wire federate, temperature and material properties. It is common for the size of the region removed, kerf width, to be assumed to be constant due to the simple geometries and relative size of errors in the manufactured geometry. In Aerospace applications however particularly in the manufacture of Unmanned Aeriel Vehicles (UAVs), these small errors can have significant impacts on aircraft behaviour and performance [1][2]. Most UAVs are designed as a combination of ruled surfaces, this makes HWC an ideal tool for manufacturing, but there design requires high geometric fidelity. Central to this challenge is the manufacture of thin geometries, when cutting thin geometries controlling the residual thermal energy after each cut becomes important. Because a HWC must make two passes near the thin trailing edge of an aerofoil the heat retained from the first pass with cause excessive ablation during the second, widening the kerf and effecting the final geometry

This paper aims to realize a method for optimizing the wire trajectory with the aim to reduce surface deviation from the target geometry. As a corollary this paper also aims to demonstrate a new method for predicting the material behaviour during thermal ablative manufacturing.

II. MOTIVATION

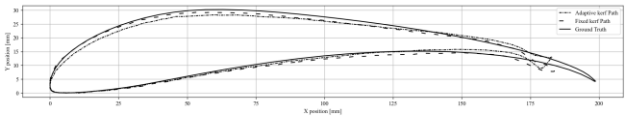

Figure 1. Processed surface geometry from foils manufactured using existing methods, S1223 Foil [3], designed chord length of 200 mm, also shown is an existing optimisation method.

Figure 1 shows processed data from a set of Two foils manufactured using existing methods to generate the machine tool paths. The scans were performed with the EINSCAN HX 3D scanner with 0.2 mm resolution [4]. The resulting data shows how the manufactured geometry deviates from the desired geometry (solid line). Over the foil surface the degree of deviation varies with the most significant losses being on the top surface and in regions of thin geometry near the fail trailing edge.

Loss of the thin geometry results in a reduced foil chord length, a reduction in foil chord can cause disproportionally large change in aerodynamic performance for the size of manufacturing error as it impacts the foils Reynolds number.

The Reynolds number describes the relative size of inertial and viscous forces in a flow and is directly proportional to wing chord, the distance from the front of a wing to the rear. Low Reynolds flows are 'thicker' and are less able change direction, for an aircraft this is important as 'thick', low Reynolds flows are less able to follow the curvature of wing surface. When the Reynolds number becomes too low or the angle of the wing relative to the oncoming flow too extreme the flow becomes detached, this phenomena is called stall, and results in a sudden loss of lift. It is clear then that a loss of foil chord directly effects when an aircraft will stall

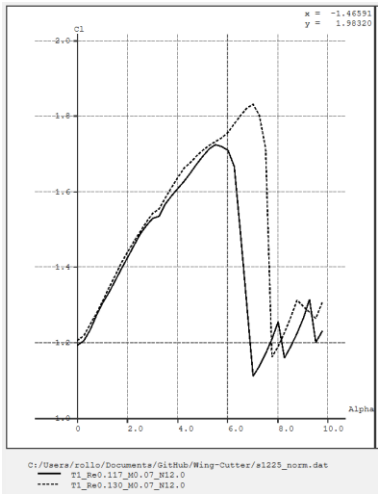

Figure 2. Results of a numerical simulation of the S1223. Shown on the X-axis is foil angle of attack, on the Y-axis is the foil lift coefficient. The results of the 2 simulations shown represent the performance of the desired geometry(dashed), and the performance of the same foil once manufacturing defects are introduced (Solid) [5]

Figure 2 shows the effect of losing 10% of air foil chord length, It can be seen that there is a reduction in both maximum lift coefficient and the angle at which lift is lost (Stall).

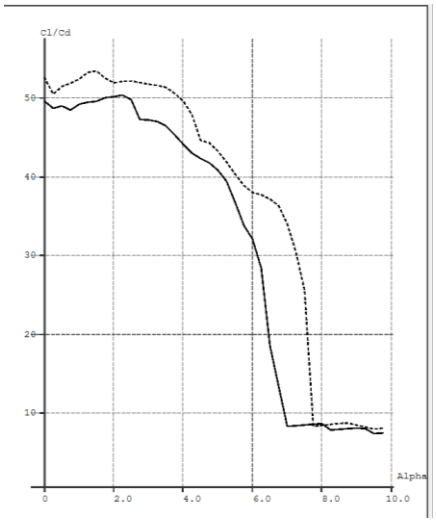

Figure 3, The results of a numerical estimation of foil efficiency for 2 different foils, with (solid) and without(dashed) manufacturing defects. On the X-axis is foil angle of attack and on the Y-axis is wing lift to drag ratio.

Figure 3 shows that a loss of this critical geometry also has implications for the efficiency of the foil, further reinforcing that small deviations in foil geometry can have disproportionate effects on flight performance and characteristics. A central goal to meet design specification results in tight margins and the need for the performance of the manufactured part to closely match the theoretical performance, we can ensure this by more closely matching the manufactured geometry to the design geometry.

Although the method used to predict foil performance cannot predict the exact performance implications of all defects and all flow features due to a limitation of degenerate based numerical estimation Cebecil show that an increase in surface roughness as

a result of environmental factors could reduces peak lift by 34% and increase drag by 6% and could induce the creation of large boundary separation bubbles [6].

Previous work by Subbiah and Karmakar has shown that the wire kerf of a HWC can be predicted numerically with high accuracy using thermal transport equations, they demonstrated that the problem can be simplified to only consider thermal coupling between the foam and wire and advection could be ignored without significantly effecting the accuracy of the prediction [7]. Although this method has credence it relies on precise knowledge of material properties and does not lend itself to use in a practical setting. The work of Subbiah and Karmakar if supported by the work of Petkov and Hattel, they directly measured wire temperature during manufacturing, although their results closely align with the later work the effect of cut curvature on the kerf width is not explored [8].

In all cases explored the authors attempt to predict the wire kerf from a known variable. This workflow is not necessarily well suited to an environment with less strict controls on material properties, and cutting conditions.

III. Aims & Objectives

The central aim of this paper is as follows:

Develop a method to optimise hotwire trajectory to reduce deviations of the manufactured part from the designed geometry.

This aim has been broken into a set of quantifiable objectives used to track progress:

OB1. Undertake a testing campaign to quantify magnitude and types of errors for fixed offset tool paths, and for the existing available methods for correcting these errors.

OB2. Research, develop and implement a new approach to address the problems identified in objective 1.

OB3. Evaluate and compare manufacturing quality, computational requirements, and implementation trade-offs.

IV. Methodology

Unlike previous methods we do not aim to predict the wire kerf, Instead we aim to predict the residual energy in the foil surface at the moment ablation stops.

The method developed is divided into 3 parts:

A. Material modelling (CSE).

For this method to work we must first robustly predict the resulting shape from a given wire trajectory. To simplify this problem, we reduce the problem to one of over or under ablation. It is assumed that at the instant ablation at a point ceases the surface specific energy, the energy per unit length will be a, known, material-dependent value, If a given surface is exposed to more thermal energy than would be required to bring it to this critical specific energy, CSE the surface will be over ablated and vice versa, it is now only necessary to calculate the cumulative surface thermal exposure at each location to determine if the final shape will be accurately produced. Although the CSE is not a analogy of a physical property it describes the behaviour or the ablation process, although a less rigorous method, it requires less precise material characterisation and provides greater robustness when material properties are not well known.

B. Thermal modelling

To compute the surface exposure both the wire trajectory and surface geometry are expressed as a composite B-Spline, $r_w(u), r_s(v)$ respectively, where $u \in [0,1], v \in [0,1]$

To simplify computation a binary mask is used to track which panels have valid interactions.

The mask is defined as:

$$\boldsymbol{R}(u,v) = \boldsymbol{r_w}(u) - \boldsymbol{r_s}(v) \quad [1]$$

$$C(u,v) = \frac{d\boldsymbol{r_s}(v)}{dv} \times \boldsymbol{R}(u,v) \quad [2]$$

$$\boldsymbol{\chi}(u,v) = \begin{cases} 1, & C(u,v) \leq 0 \\ 0, & otherwise \end{cases} \quad [3]$$

Figure 4 shows the results of this operation; black regions show what wire positions will result in ablation of which surface positions.

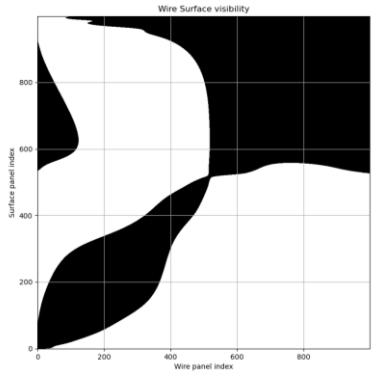

Figure 4. Wire, Surface visibility, Black regions describe regions on the surface that are visible at a chosen wire position.

The sign of value in the resulting matrix describes if a point on the wire originates from a point to the 'left' or 'right' of the corresponding point on the surface. The sign chosen is dependent on a combination of foil orientation and surface cutting direction, in the case foils are cut in an anticlockwise direction from foil Trailing edge to leading edge and back passing over the upper and then lower surfaces.

To account for variations in surface perspective and surface wire separation a perspective factor is introduced.

$$P(u,v) = \left| \frac{d\boldsymbol{r_s}}{dv} \cdot \frac{d\boldsymbol{r_w}}{du} \right| \quad [4]$$

We can now calculate the irradiance of a point on the surface because of a point on the wire trajectory.

$$e(u,v) = V(u,v) \cdot \frac{P(u,v)}{\|R(u,v)\|} \left| \frac{dr_w}{du} \right| \quad [5]$$

Each point combination is now weighted according to the relative angle between panel vectors and the separations between panels and size of each panel.

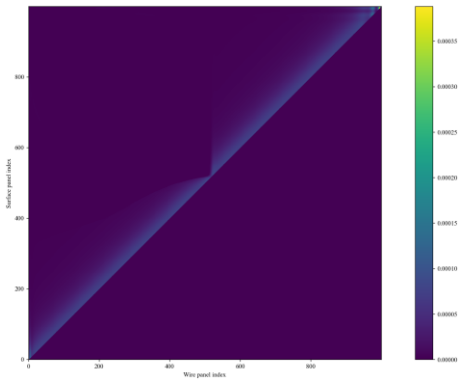

Figure 5. Wire, Surface coupling, Brighter colours represent regions of stronger coupling.

Figure 5 shows the exposure of each point on the surface because of each point along the wires trajectory; most regions experience similar heating but some regions near the trailing edge and leading-edge experience significantly more or less heating as a result of the foils geometry.

By integrating over the wire trajectory, we find the total exposure for each surface point.

$$E(v) = \int_0^1 V(u,v) \cdot \frac{P(u,v)}{\|R(u,v)\|} \left|\frac{dr_w}{du}\right| du$$

This is most clearly seen in figure 6, here we observe that the exposure varies significantly over the surface.

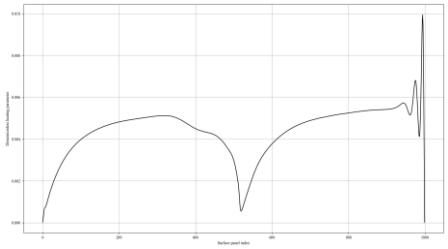

Figure 6. Panel total exposure.

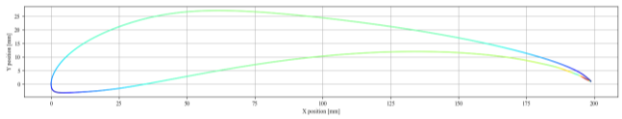

Figure 7. Superimposed panel total exposure.

Overlaying the computed exposure with the foil geometry we produce *Figure 7*. Comparing *Figure 7* to *Figure 1* it can be seen that regions with higher exposure are also the regions that most deviate from the desired geometry.

C. PSO (Particle Swarm Optimisation)

Using the developed thermal modelling method, we can now begin optimising the wire trajectory, the goal of the optimisation is for all panels to receive equal exposure.

To reduce the problem size the trajectory is converted to a Composite B-Spline. This has the effect of reducing the number of variable the optimiser must change. For this problem the optimiser will only alter the spline coefficients. To reduce the effect of Runge's phenomenon a smoothing is applied in our implementation.

The optimisation can now be stated as follows:

$$\min_{c} \mathcal{L}_{min} = \frac{1}{N}\sum_{i=1}^{N}\left(\hat{E}_I(\boldsymbol{c}, f) - CSE\right)^2$$

Subject to

$$T \cap G = \emptyset$$

Where:
$\boldsymbol{c} = \{c_0, c_1, \ldots, c_{n-1}, c_n\}$ are spline coefficients
T is the tool path
G is the surface geometry

Gradient methods such as ADAMS are not well suited to this problem as the objective function is not easily made differentiable, additionally the problem is not well bounded and the limits of the design space are not inherently known due to the B-spline representation, for these reasons PSO was chosen to optimise the design variable.

For this optimisation 20 agents are used, they are all instantiated at the same location but with different velocities, this was done due to the unknown limits of the design space. The optimisation was allowed to run for 8000 iterations with the particles re-instantiated with random velocities around the global best position every 200 iterations this was done to improve the performance of the optimiser as it often became stuck and did not further optimise without re-instantiation. Social, cognitive, and inertia weights of 0.1, 0.9 and 0.6 respectively

D. Determination of Material CSE

For Swarm-Cut to accurately reproduce the desired geometry the CSE of the material. Since the CSE cannot currently be estimated from physical properties an empirical estimation was performed.

To obtain a first order estimate of the CSE of the Expanded Polypropylene (EPP) later used in testing the same S1223 geometry was manufactured across a range of different CSE values. the chord length of each was measured and compared with the desired chord length. The CSE value corresponding to the foil whose chord most closely matched the design specification was then selected as the representative CSE for the material.

V. Optimisation Performance

Optimisation was performed on an *Intel i7-12700H* with 15.7 GB of available DDR4 system memory.

A. Optimisation performance & Time complexity

An important aspect of the use of any optimisation algorithm is the convergence performance and time complexity. Although this paper does not aim to achieve the minimum convergence time but an investigation of this implementation time complexity is felt to be valuable.

Figure 8 shows measurements of time to 15000 iterations at different degrees of discretisation. Swarm-Cut typically converges with in 8000 iterations, for this analysis the analysis was allowed to run for 15000 iterations to remove the effect of transient reduction in performance.

We ran Swarm-Cut at a range of levels of surface and trajectory discretisation, we chose 100, 200, 300, and 400 discrete points. Each discretisation level was run on 2 unique foil geometries to isolate any effects they may have had. Swarm-Cut was then run and the time to 15000 iterations timed.

Shown in figure 8 below are the results of the 8 optimisations tested, also shown is fit line

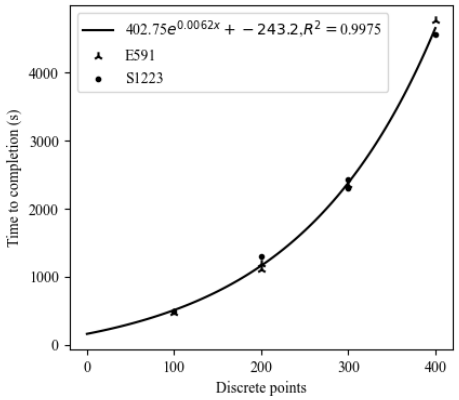

Figure 8. shows execution time data for various levels of discretisation for 2 different foil geometries.

Figure 9 shows that an exponential time complexity fits the data with a 99.8%.

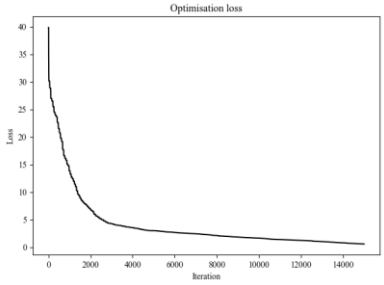

Figure 9. Plot showing optimisation loss over 15000 iterations. It is observed that the optimiser quickly converges with little stagnation between initialization and plateau.

The optimiser typically reached a plateau within 8000 iterations, as previously mentioned, a particle reinitialization step was added every 200 iterations to avoid entrapment in local minimum. Figure 9 shows typical convergence behaviour, the solution quickly converges before consistently plateauing. This provides empirical evidence for our choice of optimisation iterations and hyperparameter choices.

VI. Results

A. Theoretical results

After optimisation the predicted final heat distribution can be extracted, although this does not directly correlate with the manufactured geometry it gives a first impression on the tool path that has been found.

Below are shown the initial and optimised panel exposure distributions, both plots are plotted on the same axis. When optimising the program was tasked with achieving a CSE of 22.

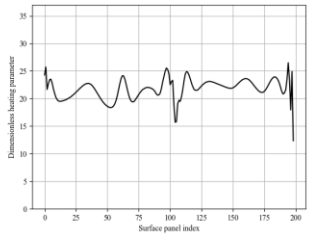

Figure 10. Optimized heating distribution

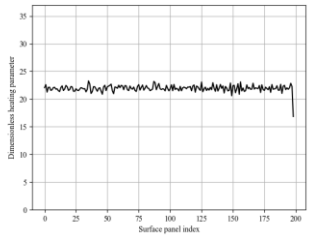

Figure 11. Optimised heating distribution, target CSE is 22

Figures 10 and 11 show clearly that the optimiser has improved the uniformity of the distribution with the exception at the later end of the cutting path. If this indirect solution reflects accurately the real-world performance the result should be that every region of the foil surfaces is left with equal exposure, if the target exposure is correctly chosen, each point on the surface will receive only the heat required to reach the desired ablation depth

B. Experimental Setup

The experimental setup involved the CNC Multitools 1610S, a control computer using MACH 3 CAM software, and an independent power supply [10].

For each test performed the machine was homed and the cutting trajectory imported from the path planning software as a G-CODE file. The cutter then moves the wire through the material following the trajectory specified. The wire moved at a consistent 200 inches per minute.

For all testing the Selig 1223 foil has been used. This foil was chosen as it has a mix of difficult geometry features, It has a very thin elongated tail and a gradually curving leading edge, these features make it a suitable benchmark for evaluating cutting accuracy.

For testing a total of 5 foils were manufactured. Two foil were manufactured using the swarm cut method, these 2 foils were chosen as initial inspection after manufacturing showed the desired geometry, at the time of manufacturing the CSE for the expanded polypropylene had not yet been found and so a range of values where tested and the foil that resulted in a foil chord closest to the desired chord was chosen. In addition smoothing was removed for one foil to investigate its effect. Although this does not represent an exhaustive testing of the effect of these 2 parameters, we believed they are a representative cross-section of swarm-cuts behaviour.

For the controls 3 methods where chosen. A fixed offset was used for the reference performance, the offset was chosen based on what machine operators believed gave the closest match to

the desired geometry. Finally 2 foils from a previous optimising program made by this author called wing-cutter were tested [9].

C. *Manufacturing results*

After manufacturing the parts were 3D scanned using the EINSCAN HX and a point cloud formed, the point clouds were first manually aligned with the reference and final alignment was performed using the Iterative Closest Point (ICP) algorithm to ensure consistency.

#	Foil	Residuals mean	Residuals std
1	CSE = 15 Smoothing = 0	-0.0109	0.3293
2	CSE = 14 Smoothing = 0.0001	-0.0090	0.2021
3	Fixed offset	-0.0088	0.2201
4	Original method corrected (OMC)	-0.0243	0.5781
5	Original method uncorrected (OMUC)	0.0129	0.2226

Table 1. Results of ICP alignment, each foil shows good alignment with the reference foils.

Table 1 shows that the final alignments had minimal error and would be able to make a valid comparison. Comparing the residual mean for the 2 foils manufactured using the CSE method we see reduced residual mean, this indicates there geometry of the foil more closely matches that of the reference foil comparing figure 12 to figure 13 we can see that figure 12 shows a closer match to the reference foil (shown in orange) than the foils manufactured using this authors previous method.

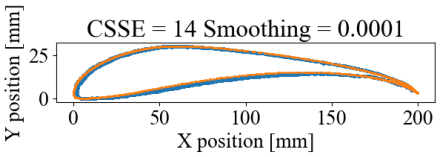

Figure 12. Comparison of a CSE method point cloud(blue), and the reference point geometry(orange)

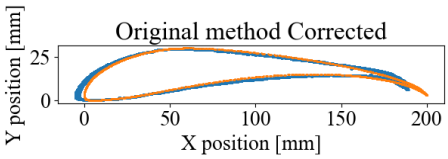

Figure 13. Comparison of the original methods point cloud(blue), and the reference point geometry(orange)

Swarm-cut also shows slightly lower residual standard deviation particularly in the case of the foil with spline smoothing, a reduced standard deviation indicates reduced surface roughness.

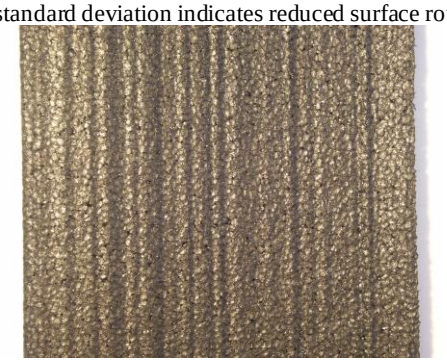

Figure 14. Lower surface of foil 1

Figure 14 shows the surface roughness of foil 1, in the figure there is a clear periodic surface defect, this is mirrored in higher residual std for this foil. Comparing this to the surface of foil 2 shown in figure 15 we can see an improved surface uniformity; this is reflected in its residual standard deviation.

Figure 15. Lower surface of foil 2

To better show the performance of each manufacturing method, the deviation between each point in a cloud and the closest reference surface was calculated. Shown below are histogram plots of the surface deviation over a representative, 9mm spanwise slice of each part scanned (the scales are preserved for ease of comparison).

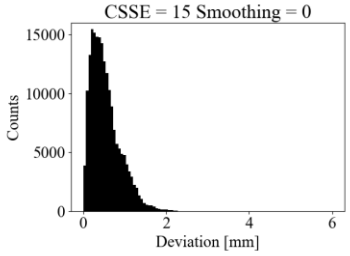

Figure 16. Surface deviation histogram for a desired critical surface energy of 15 with no spline smoothing.

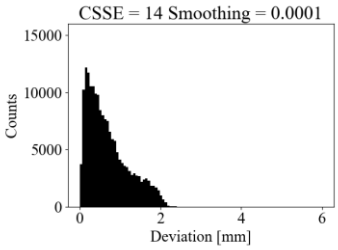

Figure 17. Surface deviation histogram for a desired critical surface energy of 14 with a spline smoothing of 0.0001.

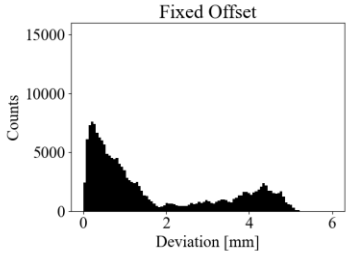

Figure 18. Surface deviation for fixed offset of 0.5mm

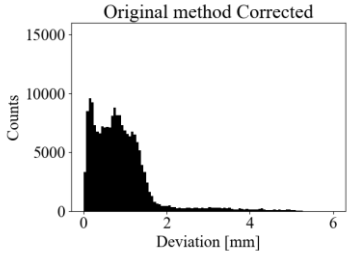

Figure 19. Surface deviation of a previous optimisation method

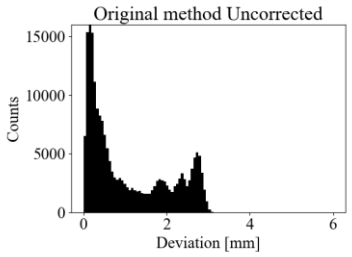

Figure 20. Surface deviation of a previous trajectory offsetting method.

The histograms above show the distribution of absolute surface deviation; each histogram contains 100 bins across a range of 0 to 6mm of surface deviation. The ideal distribution would be a single peak at zero surface deviation, and would represent a geometry where all points lie exactly on the reference surface.

Figures 16 and 17 show the new CSE method. In these histograms the surface deviation is tightly grouped within the 0 to 2mm range with figure 17 showing marginally greater dispersion. Comparing these to the remaining 3 histograms which show both a larger range and greater dispersion suggests that the CSE method is able to more accurately reproduce the desired geometry in this use case.

The table below shows the distribution of surface deviation and the improvement of each method over the traditional fixed offsetting method.

Foil	Mean [mm]	STD [mm]	Mean % change	STD % change
Fixed offset	1.674	1.592	-	-
CSE = 14 …	0.694	0.511	58.5%	67.9%
CSE = 15 …	0.531	0.352	68.3%	77.9%
OMC	0.890	0.749	46.8%	53.0%
OMUC	1.06	0.960	36.7%	39.7%

Table 2. Foil geometric accuracy and relative improvements.

Table 2 confirm the results observed in the histograms, Swarm-cut has been shown to improve geometric accuracy and smoothness. With improved determination of the material CSE it may be possible to improve accuracy further.

As described in the introduction the total length of the foil is also important, as part of the results the total length of each foil was measured and compared to the size of the desired geometry. Many of the unoptimised foils have very thin trailing edges that must be removed as it does not contribute to the foil as it has little rigidity we include both the total length and useable length in the analysis.

Foil	Chord length [mm]	usable length [mm]	% error (w/ thin)	% error
Reference	200 mm	200	-	-
Fixed offset	182 mm	170	9	15
CSE = 14 …	195 mm	195	2.5	2.5
CSE = 15	198 mm	198	1	1
OMC	182 mm	165	9	17.5
OMUC	185 mm	160	7.5	20

Table 3. Measure foil chord lengths with and without the thin trailing edge removed. Included is the percentage manufacturing error for the foil both with and without this thin trailing edge.

As with the overall geometric accuracy, Swarm-Cut shows reduced error in chord length, losing only 2 mm to 5 mm of total foil length (1 – 2.5 %) compared with a the much more significant errors with the other methods which have lost between 30 and 40 mm of material (15 – 20 %)

VII. Conclusion

The paper introduces Swarm-Cut, a PSO-based approach to hotwire cutting trajectory optimisation but formulating the optimisation problem with a new material parameter Critical Specific Energy (CSE). From the results shown about we believe we have fulfilled our central aim of reducing surface deviation. Swarm-Cut addresses the nonlinear and multivariable interactions inherent to HWC, we accomplished this by reimaging the problem as a surface energy problem and not a kerf width sizing problem.

Each of the objectives set has been met:

- Objective 1 required the quantifying error patterns in baseline and previous manufacturing methods. We accomplished this with experimental results showing the limitations of a fixed-offset and previous optimisation methods. We showed that there are 2 principle errors, loss of trailing edge, and over and under ablation.

- Objective 2 called for the development and implementation of a new approach. Swarm-Cut has met this through CSE based modelling and PSO optimisation, with demonstrable improvements in surface conformity and consistency.

- Objective 3 involved a comparative analysis of the methods examined. This was done with a quantitative evaluation of the surface mean deviation, standard deviation and chord length. We showed that Swarm-Cut outperforms other methods reducing mean surface deviation by 68.3%, a 77.9% reduction in standard deviation when compared with other methods and reduced chord length error to as low as 1%.

Swarm-Cut has demonstrated that it represents a meaningful advancement in HWC trajectory planning. Swarm-Cut integrates material properties and exposure modelling in to a simplified workflow that has been demonstrated to outperform common approaches while maintaining relative simplicity. The process developed simplifies the tuning of manufacturing parameters and lays a foundation for future work in this area of smart manufacturing.

A. Limitations and Future Work

Although we believe that the work presented provided a tangible improvement in the usability of HWCs there remain area that need further development:

1. Determination of material CSE. The current method used to determine this material specific value is not rigorous with no established framework to predict the CSE value from known material properties.

2. Optimal hyperparameter selection. The effect of spline smoothing and control point density was not sufficiently explored, it was demonstrated that use of spline smoothing has a material effect on surface quality and regularity but its interplay with CSE was not explored.

3. Complex geometries. In this paper we have focused only on simple 2D extrusions, this limits the applicability of the work performed, if Swarm-Cut is to find more widespread use the method must be generalised to more complex cutting paths.

4. Optimiser choice. The choice to use PSO was in part driven by the simplicity of the algorithm and removing the need for the solution to be differentiable, although Swarm-Cut performed well there are likely improvements to be made in the speed of convergence and ultimate performance of Swarm-Cut if a more advanced optimiser is used.

VIII. Discussion & Impact

This work presents Swarm-Cut, a Hotwire cutter trajectory optimisation method. By introducing a new parameter referred to as critical surface energy (CSE), the problem of kerf width prediction can be reformulated as a surface energy distribution problem. This approach avoid the need for thermos-mechanical characterisation of the cutting environment.

The method has shown consistent improvements to surface quality and manufacturing fidelity both in theory and in application. Reductions in both surface deviation and standard deviation show that CSE can be used to avoid the under and over ablation of material, supporting the use of CSE as a control variable in the manufacturing process

Particle Swarm optimisation (PSO) was used, this choice was made due to the non-differentiable and poorly bounded form of the objective function. Although PSO proved effective with periodic reinitialization performance, further improvements could be made using alternative methods, particularly if a differentiable objective function can be constructed.

The method presented allows improved trajectory planning in situations where material data may be unavailable or with inconsistent material properties making it more suitable to a manufacturing environment. The results presented show that optimisation based on surface energy exposure can provide measurable gains in accuracy and consistency with little added complexity.

IX. References

[1] Shum, J.G. and Lee, S., 2024. Computational Study of Airfoil Design Parameters and Sensitivity Analysis for Dynamic Stall. AIAA Journal, 62(4), pp.1611-1617. Available at: https://arc.aiaa.org/doi/full/10.2514/1.J063474 (Accessed: 02/12/24)

[2] Ceruti, A., Caligiana, G. and Persiani, F., 2013. Comparative evaluation of different optimization methodologies for the design of UAVs having shape obtained by hot wire cutting techniques. International Journal on Interactive Design and Manufacturing (IJIDeM), 7, pp.63-78.

[3] Selig, M.S. and Guglielmo, J.J., 1997. High-lift low Reynolds number airfoil design. Journal of aircraft, 34(1), pp.72-79. Available at : https://m-selig.ae.illinois.edu/pubs/GuglielmoSelig-1997-JofAC-S1223.pdf (Accessed: 02/12/24)

[4] EinScan(2024). EinScan HX. Available at : https://www.einscan.com/einscan-hx/ (Accessed: 02/12/24)

[5] XFLR5(2024). Xflr5(Verson 6.59). [Computer program]. Available at: https://www.xflr5.tech/xflr5.htm (Accessed: 02/12/24)

[6] Cebeci, T., 1987. Effects of environmentally imposed roughness on airfoil performance (No. NASA-CR-179639).

[7] Karmakar, N. and Subbiah, S., 2021. A comprehensive numerical model for kerf width prediction in hot wire cutting of expanded polystyrene. Journal of Manufacturing Processes, 61, pp.322-333. https://doi.org/10.1016/j.jmapro.2020.08.056 (Accessed: 19/05/2025)

[8] Petkov, K.P. and Hattel, J.H., 2016. A thermo-electro-mechanical simulation model for hot wire cutting of EPS foam. International Journal of Machine Tools and Manufacture, 107, pp.50-59. https://doi.org/10.1016/j.ijmachtools.2016.05.002 (Accessed; 19/05/2025)

[9] RolloTully (2025) Wing-Cutter [online]. GitHub. Available at: https://github.com/RolloTully/Wing-Cutter (Accessed: 21 May 2025).

[10] CNCMultitool. 2024. CNC Hot wire cutting machine entry series cut 1610. Available at : https://www.cnc-multitool.com/cnc-hot-wire-cutting-machine-entry-series-cut1610s.html (Accessed: 02/12/24)